Neurobiology of Aging 81 (2019) 77–87

Contents lists available at ScienceDirect

Neurobiology of Aging

journal homepage: www.elsevier.com/locate/neuaging

ABAD/17β-HSD10 reduction contributes to the protective mechanism of huperzine a on the cerebral mitochondrial function in APP/PS1 mice

Xiaodan Xiao [a,c], Qingzhuang Chen [c], Xinhong Zhu [a,**], Yong Wang [b,*]

[a] Department of Neurobiology, School of Basic Medical Science, Southern Medical University, Guangzhou, China
[b] Department of Pharmacy, Zhujiang Hospital, Southern Medical University, Guangzhou, Guangdong, China
[c] Department of Clinical Pharmacy, Guangzhou Hospital of Integrated Traditional and West Medicine, Guangzhou, China

ARTICLE INFO

Article history:
Received 10 May 2018
Received in revised form 18 May 2019
Accepted 22 May 2019
Available online 28 May 2019

Keywords:
Huperzine A
Enzyme amyloid-binding alcohol dehydrogenase
Mitochondria
β-amyloid
Tacrine

ABSTRACT

Huperzine A (HupA) is a kind of Lycopodium alkaloid with potential disease-modifying qualities that has been reported to protect against β-amyloid (Aβ)-mediated mitochondrial damage in Alzheimer's disease. However, the fundamental molecular mechanism underlying the protective action of HupA against Aβ-mediated mitochondrial malfunction is not completely understood. Recently, the mitochondrial enzyme amyloid-binding alcohol dehydrogenase (ABAD) protein has been reported to facilitate Aβ-induced mitochondrial damage, resulting in mitochondrial malfunction and cell death. Our study found that HupA, but not the acetylcholinesterase inhibitor tacrine, reduced the deposition of Aβ and the ABAD level, and further reduced Aβ—ABAD complexes, thereby improving cerebral mitochondrial function in APP/PS1 mice. This was accompanied by attenuated reactive oxygen species overload, as well as increases adenosine triphosphate levels. Moreover, HupA decreased the release of cytochrome-c from mitochondria and the level of cleaved caspase-3, thereby increasing dissociated brain cell viability in APP/PS1 mice. Thus, our study demonstrated that a reduction in ABAD was involved in the protective mechanism of HupA on the cerebral mitochondrial function in APP/PS1 mice.

1. Introduction

Alzheimer's disease (AD) is one of the most common causes of dementia, and mitochondrial dysfunction is considered to be the most representative pathophysiological response to the development of AD (Selkoe, 2007). Mitochondrial β-amyloid (Aβ) has been observed to be an essential neurotoxic species involved in the pathogenesis of AD (Readnower et al., 2011; Reddy and Beal, 2008; Rhein et al., 2009). Studies have found that the accumulation of Aβ in mitochondria causes weakened activity of the respiratory chain and a decrease in oxygen consumption in the brain of both patients with AD and transgenic APP/PS1 mouse models of AD (Caspersen et al., 2005; Dragicevic et al., 2010). Amyloid-binding alcohol dehydrogenase (ABAD), also known as 17β-HSD10 (Aitken et al., 2016), is a protein located in mitochondria and has been reported to facilitate Aβ toxicity in mitochondria of patients with AD and a mouse model of AD via the increased production of reactive oxygen species (ROS) and decreased adenosine triphosphate (ATP) levels (Lustbader, 2004; Zakaria et al., 2016).

ABAD is a unique mitochondrial enzyme that converts estrone to estradiol, which has been shown to play a pivotal role in improving cognitive function in AD. It has been shown that mitochondrial dysfunction played an important role in the pathophysiology of AD and Aβ was detected inside mitochondria and several mitochondrial proteins were found to interact directly with Aβ (Benek et al., 2015). A growing body of evidence indicates that estradiol is an essential hormone for the maintenance of mitochondrial function because it can increase mitochondrial ATP production and reduce ROS levels (Amtul et al., 2010; Grimm et al., 2012). The ABAD inhibitors have highlighted the treatment potential of AD (Benek et al., 2018; Hroch et al., 2016, 2017). Unfortunately, the increase of ABAD protein expression has been shown to exacerbate Aβ-induced mitochondrial malfunction in the brain of an AD mouse model (Lustbader, 2004; Takuma et al., 2005). The complex formed

* Corresponding author at: Department of Pharmacy, Zhujiang Hospital, Southern Medical University, Guangzhou, Guangdong, China. Tel.: +86 13424090885; fax: +86 4006014000.
** Corresponding author at: Department of Neurobiology, School of Basic Medical Science, Southern Medical University, Guangzhou, China. Tel.: +86 020-61645215; fax: +86 2154744803.
E-mail addresses: Zhuxh2005@126.com (X. Zhu), Whyong2005@126.com (Y. Wang).

0197-4580/$ – see front matter © 2019 Elsevier Inc. All rights reserved.
https://doi.org/10.1016/j.neurobiolaging.2019.05.016

by Aβ and ABAD induces abnormal ABAD structure, further preventing the binding of ABAD to NAD+, which results in ABAD's inability to exert enzymatic activity (Lustbader, 2004). However, Aitken et al. (2017) found that the use of a small-molecule inhibitor of the ABAD protein improved the function of neuronal mitochondria and alleviated the symptoms of AD. In addition, Lustbader (2004) used an ABAD decoy peptide (ABAD-DP) to antagonize the combination of Aβ and ABAD, and to protect mitochondrial function in neurons from Tg ABAD mice. Therefore, decreasing the level of ABAD could be a promising potential strategy for the treatment of AD.

Huperzine A (HupA), a Lycopodium alkaloid from *Huperzia serrata* (Qian Ceng Ta), is a safe, potent inhibitor of acetylcholinesterase (AChE) that has potential disease-modifying properties in the treatment of AD (Zhu et al., 2015). HupA has been widely used for the treatment of AD and other forms of dementia in China for decades, and clinical trials have been conducted in the United States to test its ability to treat dementia-related disease (http://www.clinicaltrials.gov/show/NCT00083590). Interestingly, it has been reported that HupA can attenuate Aβ-mediated neurotoxicity through a non–AChE inhibitor (AChEI)-dependent pathway in various AD mouse models (Lei et al., 2015; Zhang, 2012). Because AD is a multicausal neurodegenerative disease, it is very important to investigate the non-AChEI-dependent mechanism of action of HupA to better guide its clinical application and to develop HupA-derived drugs. Our previous study demonstrated that HupA-pretreated neural stem cells were protected from Aβ-induced apoptosis in a microglial–neural stem cell coculture system (Zhu et al., 2015). Moreover, a growing number of studies show that HupA protects against Aβ-induced brain mitochondria malfunction and significantly increases primary cortical neuron and neural stem cell survival (Chen and Yan, 2007; Gao et al., 2009; Zhu et al., 2015). However, the essential mechanisms underlying the protective effects of HupA against Aβ-mediated neurotoxicity in AD have not been comprehensively explored. Owing to the reported increase in the ABAD–Aβ complexes as a response to enhanced mitochondrial stress in the brain of Tg mAPP AD and Tg mAPP/ABAD mouse models (Lustbader, 2004; Takuma et al., 2005), and protective effects of HupA against Aβ-induced mitochondrial dysfunction, we investigated the role of the ABAD in the protection of mitochondria. Our present work offers new insights into the mechanism underlying ABAD-dependent mitochondrial protection of HupA.

2. Materials and methods

2.1. Animals and drug administration

Male APPswe/PS1dE9 mice (APP/PS1, 20–30 g) obtained from the Nanjing Model Animal Research Center (MARC, China) were used as an AD mouse model. Mouse tail biopsies were subjected to PCR analysis to verify the genotype. The animals were maintained under standard laboratory conditions (12 hours light–dark cycle with lights on from 7:00 a.m. to 7:00 p.m.; free access to food and water). The age-matched wild-type (WT) mice were used as controls. All animal studies were performed in accordance with the Regulations for the Administration of Affairs Concerning Experimental Animals (China) and were approved by the Institutional Animal Care and Use Committee of Southern Medical University (China).

HupA (Wan Bang Pharmaceutical, China) was dissolved in 0.1 M HCl as stock solution and then diluted with physiological saline before administration. The final concentration of HCl and pH for huperzine for the injection of mice was 10^{-6} M and 6.5, respectively. Tacrine (an AChEI) hydrochloride hydrate (Sigma, USA) was dissolved in physiological saline solution. It was used to better illustrate that the mitochondrial protection of HupA is independent of AChE inhibition. Experiments were carried out using the following groups: (1) APP/PS1-HupA group: APP/PS1 mice at 2 months of age were subjected to intraperitoneal (*i.p.*) administration of HupA (0.1 mg/kg) every day for 6 months before being killed (Huang et al., 2014); (2) WT-HupA group: age-matched WT mice were treated as described previously; (3) APP/PS1-vehicle group: APP/PS1 mice at 2 months of age were subjected to *i.p.* administration of physiological saline every day for 6 months before being killed; (4) WT-vehicle control group: age-matched WT mice were treated like the APP/PS1-vehicle group; (5) APP/PS1-tacrine group: APP/PS1 mice at 2 months of age were subjected to *i.p.* administration of tacrine (0.5 mg/kg) every day for 6 months before being euthanized.

2.2. Preparation of $A\beta_{1-42}$ peptide

$A\beta_{1-42}$ was purchased from Invitrogen (USA) and prepared according to previous methods (Chen et al., 2016). Briefly, $A\beta_{1-42}$ was dissolved in HPLC-grade water, followed by the addition of phosphate-buffered saline (PBS, 10 mM). The peptide solution was incubated at 37 °C for 24 hours and then stored at −20 °C.

2.3. Preparation of dissociated brain cells

Dissociated brain cells (DBCs) were prepared as previously described (Abdel-Kader et al., 2007; Asseburg et al., 2016; Pohland et al., 2018; Stoll et al., 1992) with a slight modification. Briefly, mice were killed and their brains were extracted on ice. The meninges, capillaries, and cerebellum were removed, and one of the 2 cerebral hemispheres was washed with ice-cold medium I (138 mM NaCl, 5.4 mM KCl, 0.17 mM Na_2HPO_4, 0.22 mM K_2PO_4, 5.5 mM glucose, and 58.4 mM sucrose; pH 7.35). The cerebrum was diced with a sterile razor blade. Tissues were dissociated in Dulbecco's modified Eagle's medium/Ham's F12 nutrient mixture (DMEM/F12) (Gibco, USA) containing 0.25% trypsin-EDTA (Gibco, USA), incubated at 37 °C for 15 minutes, and shaken every 5 minutes. Next, trypsin activity was blocked with the addition of DMEM/F12 supplemented with 10% fetal bovine serum (Gibco, USA). Cell suspensions were then collected by centrifugation at 1000 × *g* at 4 °C for 5 minutes. The pellet was resuspended in medium II (110 mM NaCl, 5.3 mM KCl, 1.8 mM $CaCl_2 \cdot H_2O$, 1 mM $MgCl_2 \cdot 6H_2O$, 25 mM glucose, 70 mM sucrose, and 20 mM HEPES; pH 7.4) and washed twice. Then the acutely prepared DBCs were used for measurements of ROS levels, ATP production, and cytochrome release. To observe the morphology of DBCs and to perform the 3-(4,5-Dimethylthiazol-2-yl)-2,5-diphenyltetrazolium bromide (MTT) and lactate dehydrogenase (LDH) assay, DBCs must be seeded into a poly-L-lysine (0.01%) precoated plate to allow the cells to adhere to the wall and then undergo subsequent testing procedures. Cell morphology and proliferation curve was shown in Supplement Fig. 1. Protein concentration was determined using the BCA protein assay kit (Thermo Fisher Scientific, USA). Finally, the other cerebral hemisphere was stored at −80 °C.

2.4. PC12 cell culture

PC12 cells were purchased from the American Type Culture Collection (ATCC, USA). These cells were used to explore the effects of Aβ on mitochondrial ABAD protein level in neuronal cells. Briefly, PC12 cells were cultured in 25-cm^2 cell culture flasks at a concentration of 5 × 10^5 cells/cm^2 in complete medium (RPMI-1640 medium [Gibco, USA] containing 10% fetal bovine serum [Gibco, USA]). The in vitro experiments were conducted at a passage number of approximately 6–15.

2.5. Acetylcholinesterase (AChE) activity assay

The activity of AChE was assayed according to previously described methods (Ellman et al., 1961). Briefly, cerebral homogenates from each group were incubated with 10 mM butyryl cholinesterase inhibitor and tetraisopropyl pyrophosphoramide iso-OMPA (Sigma, USA) for 1 hour. AChE activity was measured using a colorimetric AChE assay kit (Abcam, USA) according to the manufacturer's instructions. Data are expressed in μmol/min/mU.

2.6. 3-(4,5-Dimethylthiazol-2-yl)-2,5-diphenyltetrazolium bromide (MTT) and lactate dehydrogenase (LDH) assays

MTT (Sigma, USA) and LDH assay kits (Abcam, USA) were utilized to evaluate the neuroprotective effects of HupA on DBCs viability in APP/PS1 mice. Assays were carried out according to the manufacturer's protocols.

MTT assays were performed as previously described (Chen et al., 2016) with a slight modification. Briefly, acutely prepared DBCs were seeded into poly-L-lysine precoated 96-well plates (2×10^4 cells per well) and incubated in culture medium (DMEM/F12 supplemented with 10% fetal bovine serum) for 24 hours in a typical 37 °C humidified cell-culture incubator containing 5% CO_2 and 95% air. After washing 3 times with PBS, the MTT solution (10 μL, 5 mg/mL) was added to the wells, and the cells were incubated at 37 °C for 4 hours. After removing the supernatant, dimethyl sulfoxide (100 μL) (Sigma, USA) was added to the wells, and the absorbance at 590 nm was measured with an automated microtiter plate reader.

The LDH assay was performed according to the manufacturer's protocols. Briefly, after the acutely prepared DBCs were seeded into poly-L-lysine precoated 96-well plates (2×10^4 cells per well) for 24 hours, the supernatant was harvested to test the LDH release. To detect the total LDH activity, DBCs were seeded into poly-L-lysine precoated 96-well plates (2×10^4 cells per well) for 24 hours, then Triton X-100 (10%) was added to incubate for 1 hour in the incubator, and the supernatant was collected for testing. The activity of LDH was detected by recording the change in NADH concentration after adding a colorimetric probe to the supernatant for 1 hour. The absorbance at 490 nm was measured with an automated microtiter plate reader. The results were calculated by dividing the average LDH release value of test by the average total LDH release value using the following formula: LDH (%) = (LDH release of test/total LDH) × 100.

2.7. Detection of ROS levels

ROS were determined using dihydrorhodamine 123 (DHR) (Invitrogen, USA) as previously described (Abdel-Kader et al., 2007) with a slight modification. DHR, an uncharged and nonfluorescent indicator, passively diffuses across membranes, where it is oxidized to cationic rhodamine 123, which localizes in the mitochondria and displays green fluorescence. First, acutely prepared DBCs were seeded into 48-well plate (1×10^5 cells per well); subsequently, 5 μM DHR was added to each well, and the cells were incubated for another 30 minutes. After washing twice with PBS, fluorescence was measured using an automated microtiter plate reader (excitation at 488 nm and emission at 515 nm). Protein concentration was determined using a BCA kit, and values were normalized to the amount of protein.

2.8. Detection of ATP production

ATP levels were measured using a bioluminescent ATP assay kit (Promega, USA) according to the manufacturer's instructions with a slight modification. Briefly, acutely prepared DBCs from each group were lysed by the addition of 100 μL of ATP-releasing reagent. Then, luciferin substrate and luciferase enzyme were added to the lysates and incubated for 10 minutes in the dark, and bioluminescence was assessed on a PerkinElmer microplate reader (PerkinElmer, USA). Bioluminescence intensity was normalized to the control group and reported as the relative ATP level (Cha et al., 2012).

2.9. Immunocytochemical staining of ABAD

To investigate the effect of Aβ on mitochondrial ABAD protein level in PC12 cells, experiments were performed using the following groups: (1) Control: PC12 cells were cultured in complete medium for 24 hours; (2) Aβ: PC12 cells were treated with $A\beta_{1\text{-}42}$ (1 μM) for 24 hours; (3) Aβ-HupA: PC12 cells were pretreated with HupA (10 μM) for 1 hour, followed by the addition of $A\beta_{1-42}$ (1 μM) and incubation for another 24 hours; (4) HupA: PC12 cells were treated with HupA (10 μM) for 24 hours; (5) Aβ-Tacrine: PC12 cells were pretreated with tacrine (1 μM) for 1 hour, followed by the addition of $A\beta_{1-42}$ (1 μM) and incubation for another 24 hours. Briefly, cells growing on coverslip were fixed in 4% paraformaldehyde for 15 minutes and incubated with anti-ABAD antibody (ab10260, 1:500; Abcam, USA) at 4 °C overnight, followed by DyLight 488 AffiniPure Goat Anti-Rabbit IgG secondary antibody (A23220, 1:5000; Abbkine, USA) at 37 °C for 1 hour in the dark. Images were visualized with a microscope (Olympus, Japan). Band analysis was performed using ImageJ 1.43m software (National Institutes of Health).

2.10. Analysis of cytochrome c release

To determine the effect of HupA on the release of cytochrome c from the mitochondria to the cytoplasm in DBCs, cytochrome c release was measured as previously described (Lustbader, 2004) with a slight modification. Briefly, after washing twice with PBS, acutely prepared DBCs from each group were collected by centrifugation at 300 × *g* for 5 minutes at 4 °C. The pellet was resuspended in 400 μL of lysis buffer (50 mM Tris at pH 7.4, 1 mM EDTA, 1 mM EGTA, 250 mM sucrose, 2 μg/mL leupeptin, 1 mM PMSF, and 1 μg/mL pepstatin A) and lysed with 10 strokes of a Dounce homogenizer. Cytosol and membrane fractions were separated by centrifugation at 105,000 × *g* for 1 hour at 4 °C. The supernatants were harvested and then concentrated to 20 μL, whereas the pellets were mixed with 50 μL of lysis buffer. The protein concentration of each fraction was determined by the bicinchoninic acid assay (Thermo Scientific Pierce, USA). Samples (30 μg) were subjected to Western blotting using an antibody to cytochrome c (#4272, 1:1000; Cell Signaling Technology, UK) followed by a horseradish peroxidase-conjugated goat anti-rabbit IgG secondary antibody (111-035-047, 1:5000; Abbkine, USA).

2.11. Western blotting

Cerebra were homogenized in ice-cold extraction buffer (10 mM Tris–HCl [pH 7.4], 100 mM sodium chloride, 1 mM EDTA, 1 mM EGTA, 1 mM sodium fluoride, 20 mM sodium pyrophosphate, 2 mM sodium orthovanadate, 1% Triton X-100%, 10% glycerol, 0.1% sodium dodecyl sulfate [SDS], and 0.5% deoxycholate) supplemented with a protease inhibitor cocktail (phosphatase inhibitors, protease inhibitor, 1 mM phenylmethylsulfonyl fluoride) (Sigma, San Francisco, CA, USA). BCA protein assay kit (Thermo Scientific Pierce, USA) was used to determine protein concentration. Equal amounts (20 μg) of protein samples were separated on 12% SDS-polyacrylamide gels (Sigma, USA) and then transferred onto 0.2 μm polyvinylidene difluoride membranes (Thermo Scientific Pierce, USA). Membranes were blocked at room temperature for 1 hour with 5% (wt/vol)

nonfat milk in tris buffered saline Tween (20 mM Tris HCl, 150 mM sodium chloride, and 0.1% Tween-20). Thereafter, the membranes were incubated with primary antibodies at 4 °C overnight, followed by the corresponding secondary antibodies for 1 hour at room temperature. The following antibodies were used in this experiment: mouse monoclonal anti-ABAD (ab10260, 1:1000, Abcam, USA), 6E10 monoclonal antibody (SIG-39320, 1:1000, Covance, USA), mouse monoclonal anti-β-actin (ab8226, 1:2000, Abcam, USA), rabbit monoclonal anti-active caspase-3 (ab32042, 1:500; Abcam, USA), and horseradish peroxidase-conjugated goat anti-rabbit IgG (111-035-047, 1:5000, Abbkine, USA). Band analysis was executed using ImageJ 1.43m software. β-Actin was used as a loading control.

2.12. Thioflavin S immunostaining

Thioflavin S staining was performed as previously described (Heneka et al., 2012) with a slight modification. Animals were deeply anesthetized with 10% chloral hydrate and transcardially perfused with 0.9% saline containing heparin (10 U/mL). The brains were removed and fixed in 4% paraformaldehyde solved in 0.1 M PBS (pH 7.4) for 4 hours. Fixed brains were immersed in 30% sucrose for 48 hours, and 6 × 6 series of coronal frozen sections (40 μm) containing the hippocampus were cut on a vibratome (Leica, Germany). For thioflavin S (Sigma, USA) immunostaining, slices were incubated in 0.1% thioflavin S (in 50% alcohol) for 8 minutes and washed 3 times for 3 minutes with 50% alcohol, followed by mounting. Images with fluorescence were captured by confocal microscope (Olympus, Japan). Total plaque number and Aβ area fraction were calculated using the software ImageJ 1.43 m with plugins from the WCIF ImageJ collection. In particular, images were normalized and an automatic thresholding on the basis of the entropy of the histogram ("MaxEntropy") was used to identify the plaques. Finally, plaque number, plaque area, and average Aβ plaque size were calculated using the "analyze particles" plugin of ImageJ. The Aβ area fraction was determined by dividing total plaque area by the area of the microscopic field.

2.13. Isolation of brain mitochondria

To obtain highly purified mitochondria for the coimmunoprecipitation/immunoblotting assay, mitochondria from the cerebra of each group was isolated using a Tissue Mitochondria Isolation Kit, according to the manufacturer's instructions (Beyotime, China). Briefly, cerebra from each group were added to isolation buffer (1 mM EDTA and 20 mM HEPES at pH 7.2) and then homogenized with 10 strokes of a Dounce homogenizer. The resulting homogenate was spun at 1500 × *g* for 5 minutes at 4 °C. The supernatant was collected and then centrifuged at 12,000 × *g* for 30 minutes at 4 °C. The resulting pellet consisted of highly purified mitochondria.

2.14. Immunoprecipitation/immunoblotting for detection of ABAD-Aβ complex

We used highly purified mitochondria to perform immunoprecipitation/immunoblotting as previously described (Lustbader, 2004) with a slight modification. Briefly, brain mitochondria were resuspended in Tris buffer (10 mM Tris, 0.1 M NaCl, 1 mM EDTA, 100 μg/mL PMSF, 1 μg/mL aprotinin, protease inhibitors mixture) (Sigma, USA) and then centrifuged at 14,000 × *g* for 5 minutes at 4 °C. The resulting supernatant was immunoprecipitated with rabbit anti-Aβ IgG (SIG-39320, 6E10, 1:1000; Covance) at 4 °C overnight, followed by incubation with protein A/G beads (Thermo Scientific Pierce, USA) for 2 hours at 20 °C. The resulting immunoprecipitate was subjected to immunoblotting using a mouse antibody to ABAD (1:1000; Abcam, USA). Horseradish peroxidase-conjugated goat anti-rabbit IgG (1:5000; Abbkine, USA) was used as a secondary antibody.

2.15. ELISA quantification of Aβ

Mice were deeply anesthetized and perfused with 0.9% saline. The brains were removed from the skull and frozen immediately for biochemical analysis. Briefly, cerebra were homogenized in 2% SDS with protease inhibitors, centrifuged at 100,000g for 1h at 4 °C and the pellet containing insoluble Aβ was extracted with 70% formic acid in water. Formic acid extracts were neutralized initially by 1:20 dilution into 1 M Tris phosphate buffer, pH 11. Quantitative determination of Aβ was performed using a solid-phase sandwich enzyme-linked immunosorbent assay (ELISA) kit (Invitrogen) for the determination of $A\beta_{1-40}$ and $A\beta_{1-42}$ according to the protocol of the supplier. Briefly, 50 μL standard Aβ of gradient concentration and protein samples was added to the Aβ antibody-bedded plate, and 50 μL detection antibody was added next. After incubation overnight at 4 °C, the liquid was discarded and the wells were washed 4 times at least for 30s. Then the wells were incubated in 100 μL Anti-Rabbit HRP working solution for 30 minutes at room temperature followed by 100 μL stabilized chromogen incubation for 30 minutes at room temperature in the dark. 100 μL stop solution was added and the absorbance of each well was read at 450 nm. A 4 parameter algorithm was used for standard curve fitting and sample Aβ concentration was calculated.

2.16. Statistics

Statistical analysis was performed using SPSS version 20.0 software. A one-way analysis of variance was used to test statistically significant differences between experimental groups, followed by the post hoc Tukey's multiple comparisons test. All of the data were expressed as mean ± standard error of the mean (SEM), and statistical significance was considered as $p \leq 0.05$.

3. Results

3.1. HupA treatment attenuated mitochondrial dysfunction in APP/PS1 mice

Numerous studies have demonstrated that binding of Aβ to ABAD leads to mitochondrial damage, including ROS overload and decreased ATP levels. Therefore, the aforementioned parameters were detected in this study to comprehensively evaluate the protective effect of HupA on the mitochondria of APP/PS1 mice.

Mitochondria are the principal source of ROS generation. The overproduction of ROS causes mitochondrial damage and cell apoptosis (Volobouevaet al., 2010). Previous studies have shown that Aβ triggers oxidative stress in mitochondria, such as mitochondrial calcium ion overload (Sanz-Blasco et al., 2008), mitochondrial DNA defects (Hirai et al., 2001), and complexes formed by Aβ and ABAD (Pagani and Eckert, 2011). This promotes leakage of ROS and causes mitochondrial dysfunction and cell death (Lustbader, 2004). Consequently, we assessed whether the mitochondrial neuroprotective effect of HupA was accompanied by decreased generation of ROS. As shown in Fig. 1A, compared with the WT-vehicle group, the APP/PS1 group demonstrated a significantly higher DHR fluorescent intensity ($p < 0.01$), and the administration of HupA to APP/PS1 mice markedly reduced DHR fluorescent intensity ($p < 0.01$) compared with APP/PS1 mice without HupA. However, tacrine, an AChE inhibitor, did not significantly reduce DHR fluorescence intensity compared with APP/PS1 mice ($p > 0.1$). In addition, HupA treatment alone did not

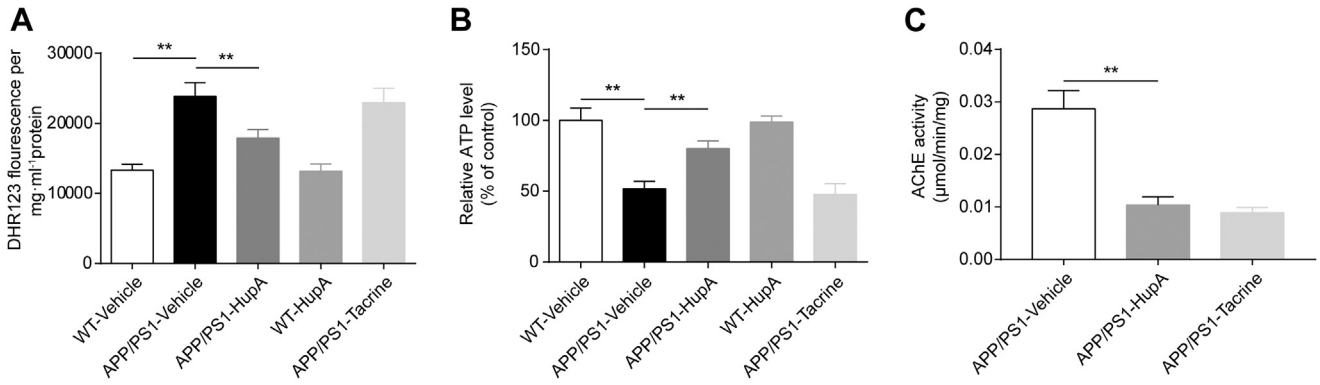

Fig. 1. Huperzine A exerted a protective effect on mitochondrial function in DBCs. (A) DHR 123 was used as an ROS indicator and added to each well of DBCs. Fluorescence was measured using a microtiter plate reader normalized to the protein amount (n = 5). (B) ATP levels were detected using a bioluminescent ATP assay kit (n = 6). DBCs from each group were lysed, luciferin substrate and luciferase enzyme were added to the lysates and incubated for 10 minutes in the dark, and bioluminescence was assessed on a microplate reader. Bioluminescence intensity was normalized to the control group and reported as the relative ATP level. (C) Cerebral homogenates from each group were incubated with 10 mM butyryl cholinesterase inhibitor and tetraisopropyl pyrophosphoramide iso-OMPA for 1 hour. AChE activity was measured using a colorimetric AChE assay kit, and the data are expressed in μmol/min/mU (n = 4). $^{**}p < 0.01$. Abbreviations: AChE, acetylcholinesterase; ATP, adenosine triphosphate; HupA, huperzine A; WT, wild-type; DBCs, dissociated brain cells; ROS, reactive oxygen species; DHR, dihydrorhodamine 123.

change the DHR fluorescent intensity in WT mice compared with the WT-vehicle control group ($p > 0.1$).

Because ATP levels are strongly associated with mitochondrial activity (Liu et al., 2005), the level of ATP was used to evaluate mitochondrial function in the brains of APP/PS1 mice with or without HupA. We observed that the ATP level of the APP/PS1-vehicle group was reduced markedly compared with the WT-vehicle group ($p < 0.01$, Fig. 1B); interestingly, this decrease was partially inhibited by treatment with HupA in the APP/PS1 mice ($p < 0.01$, Fig. 1B) but not by tacrine ($p > 0.1$, Fig. 1B). There was no significant difference between the WT-vehicle control group and WT-HupA group ($p > 0.1$, Fig. 1B).

To determine whether the level of AChE inhibition by HupA is equivalent to that induced by tacrine, the activity of AChE in HupA- or tacrine-treated APP/PS1 mice was evaluated using a colorimetric AChE assay kit. The results showed no significant difference in AChE activity between HupA-treated APP/PS1 mice and tacrine-treated APP/PS1 mice ($p > 0.1$, Fig. 1C).

Taken together, the aforementioned results confirm that the protective effects of HupA on mitochondria in APP/PS1 mice is mediated by decreased levels of ROS and increased ATP.

3.2. HupA decreased the level of Aβ in APP/PS1 mice

Many studies have shown that the $A\beta_{1-42}$ oligomer morphology is the most toxic form of Aβ and has a significant connection to the pathological changes of AD (Sakono and Zako, 2010). We therefore analyzed the effect of HupA or tacrine on $A\beta_{1-42}$ oligomer level and deposition of Aβ in the APP/PS1 mice using Western blotting and thioflavin S staining techniques. The brains of the APP/PS1 mice showed greatly increased levels of $A\beta_{1-42}$ oligomers (~27 kDa, a form with high neurotoxicity) compared with the age-matched WT control group ($p < 0.001$, Fig. 2A and B). HupA treatment vastly decreased the $A\beta_{1-42}$ oligomer level in the APP/PS1 mice ($p < 0.001$, Fig. 2A and B and Supplement Fig. 2), whereas the tacrine-treated group failed to exert this effect ($p > 0.1$, Fig. 2A and B). In addition, aggregated forms of Aβ in the APP/PS1 mice treated with HupA were further analyzed by ELISA. As shown in Fig. 2F, there was a strong reduction of $A\beta_{1-40}$ and $A\beta_{1-42}$ in both cortex and hippocampus tissues in APP/PS1 mice treated with HupA after sequential extraction by SDS and formic acid buffer. Similarly, thioflavin S (Sigma, USA) staining showed a marked decrease in hippocampal and cortical Aβ deposition in the HupA-treated APP/PS1 mice but not in tacrine-treated APP/PS1 mice ($p > 0.1$, Fig. 2C–E). These results indicate that HupA treatment contributed to the decrease of Aβ levels in APP/PS1 mice.

3.3. Effect of HupA on ABAD protein levels

Studies have shown that the ABAD protein is directly associated with Aβ-mediated mitochondrial dysfunction and cell death (Lustbader, 2004). Therefore, we determined ABAD protein levels by Western blotting using an anti-ABAD antibody. As shown in Fig. 3, ABAD levels were increased in the APP/PS1 mice compared with those of the WT-vehicle control group ($p < 0.001$, Fig. 3A and B). Interestingly, treatment with HupA markedly reduced ABAD levels ($p < 0.001$, Fig. 3A and B) compared with the APP/PS1 group, and no significant difference was observed between the WT-vehicle control group and the WT-HupA group, or between the APP/PS1-HupA group and APP/PS1-tacrine group ($p > 0.1$, Fig. 3A and B). Moreover, ABAD protein levels were also elevated in PC12 cells treated with $A\beta_{1-42}$ (1 μM) in vitro compared with the control group, whereas pretreatment with HupA but not tacrine attenuated the ABAD levels compared with the Aβ group ($p < 0.001$, Fig. 3C and D). Together, these results demonstrate that HupA decreased mitochondrial ABAD levels in APP/PS1 mice in vivo and in PC12 cells in vitro.

3.4. HupA reduced the level of ABAD complexes

To further investigate whether HupA reduces the level of ABAD–Aβ complexes, we measured the ABAD–Aβ compound in APP/PS1 mice brain by immunoprecipitating cerebral mitochondria protein extracts with anti-Aβ and subsequently subjecting them to immunoblotting with anti-ABAD immunoglobulin G. We found that APP/PS1 mice displayed a vast increase of the ABAD–Aβ complex level compared with the age-matched WT control group ($p < 0.001$; Fig. 4), and HupA treatment significantly reduced the levels of ABAD–Aβ complex ($p < 0.001$; Fig. 4). Nevertheless, the tacrine-treated group did not show a significant decrease in ABAD–Aβ complex levels ($p > 0.1$; Fig. 4). The findings suggest that HupA is associated with decreased levels of mitochondrial ABAD–Aβ complexes in the brain of APP/PS1 mice.

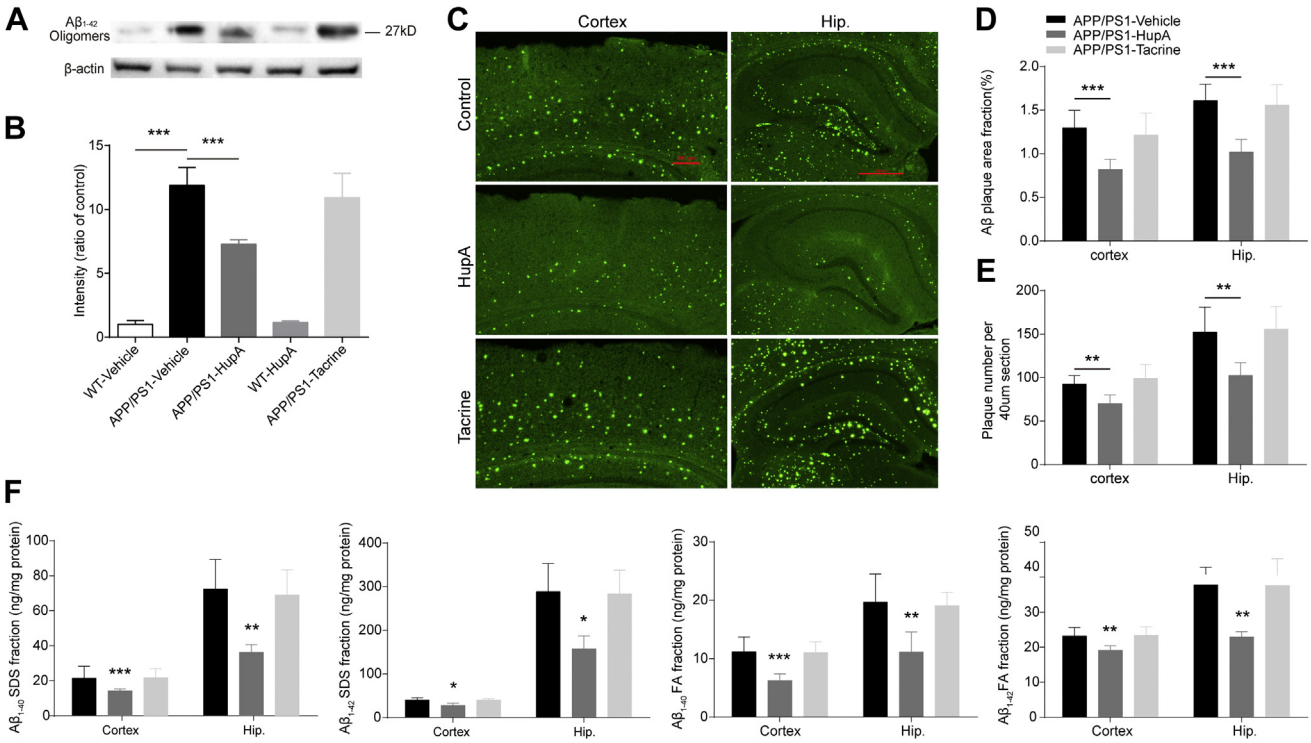

Fig. 2. HupA decreased amyloid-β deposition. (A) Representative images of $A\beta_{1-42}$ oligomers in the brain tissue from one mouse of each group were analyzed by Western blotting; β-actin served as an internal control. (B) Quantification of the densitometry of $A\beta_{1-42}$ oligomer intensity from all experimental groups. (C) Aβ plaque deposition was quantified in the hippocampus (Hip.) and cortex using thioflavin S. (D–E) Quantification of the number and surface area of Aβ plaques was performed in 6 consecutive sections per animal; data are expressed as count per area or area fraction (%). (F) ELISA of SDS and FA fractions for $A\beta_{1-40}$ and $A\beta_{1-42}$ from 8-month-old mice. (n =6, mean ± SEM, $^{*}p < 0.05$, $^{**}p < 0.01$,$^{***}p < 0.001$. Abbreviations: Aβ, β-amyloid; HupA, huperzine A; ELISA, enzyme-linked immunosorbent assay; FA, formic acid; SDS, sodium dodecyl sulfate.

3.5. HupA decreased cytochrome c release and cleaved caspase-3 levels in the brain of APP/PS1 mice

Cytochrome c, a protein with apoptogenic potential that is released from the mitochondrial intermembrane space into the cytoplasm, can trigger a caspase-dependent apoptosis cascade (Pagani and Eckert, 2011; Takuma et al., 2005). To clarify whether HupA is involved in the regulation of cytochrome c protein levels in the DBCs of APP/PS1 mice, a cytochrome c primary antibody was used to analyze the distribution of cytochrome c in the cytoplasm and mitochondrial matrix by immunoblotting. As shown in Fig. 5, the APP/PS1-vehicle group suffered a loss of cytochrome c from the mitochondrial or membrane fraction to the cytosol fraction ($p < 0.001$, Fig. 5A), and HupA treatment partially prevented this release in the APP/PS1 mice ($p < 0.01$, Fig. 5A). However, tacrine treatment did not effectively restrain cytochrome c release from the mitochondria to the cytoplasm ($p > 0.1$, Fig. 5A).

Because cytochrome c can induce the cleavage of caspase-3, subsequently activating the caspase-3-dependent apoptotic response (Halestrap, 2005), we used a cleaved caspase-3 antibody

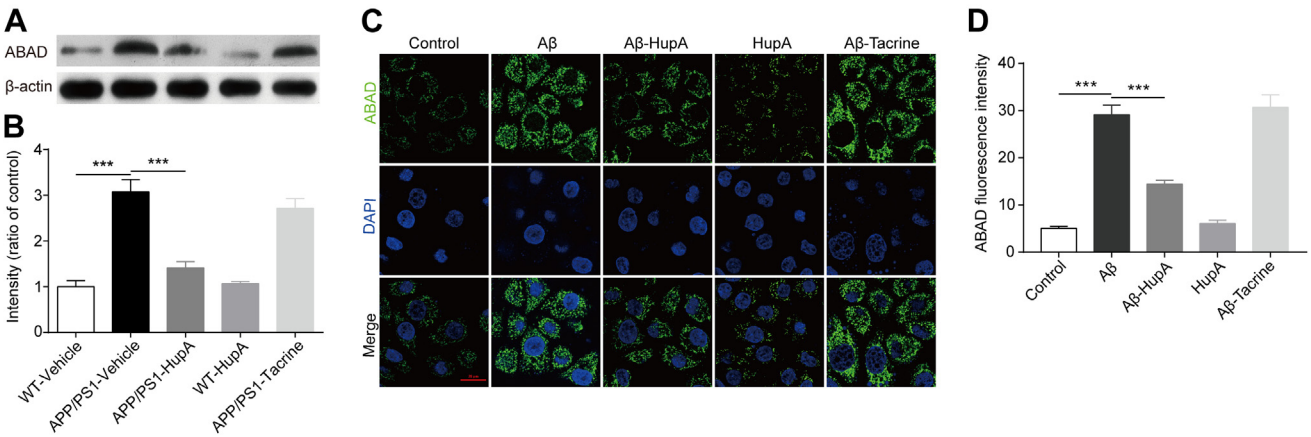

Fig. 3. Effect of HupA on ABAD protein levels. (A) Representative images of western-blot showing the ABAD expression in the brain tissue of one mouse from each group, β-actin served as an internal control. (B) The densitometry of ABAD intensity from all of the experimental groups. (C) Representative images of ABAD immunocytofluorescence staining of PC12 cells. PC12 cells were pretreated with HupA (10 μM) or Tacrine (1 μM) for 1 hour, followed by treatment with $A\beta_{1-42}$ (1 μM) for 24 hours. Green fluorescence represents the ABAD protein; blue fluorescence represents the nucleus of PC12 cells. Images are representative of 3 independent experiments. Scale bar = 20 μm. (D) Quantitative analysis of the green fluorescence intensity. $^{***}p < 0.001$. Abbreviations: Aβ, β-amyloid; HupA, huperzine A; ABAD, amyloid-binding alcohol dehydrogenase. (For interpretation of the references to color in this figure legend, the reader is referred to the Web version of this article.)

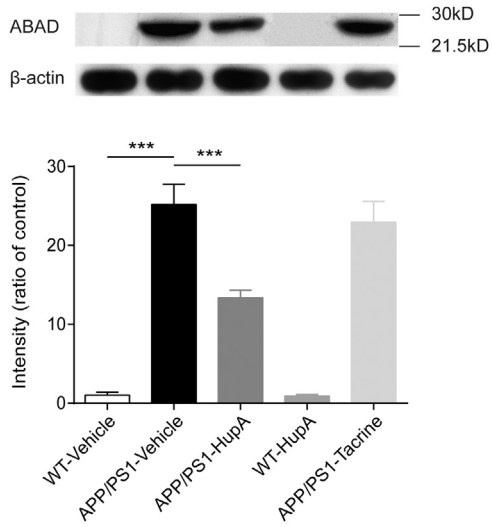

Fig. 4. Effect of HupA on ABAD–Aβ association in APP/PS1 mice brain. Mitochondria were purified from brain tissues of the mice in each group. The ABAD–Aβ complex in APP/PS1 mice was determined by immunoprecipitating cerebral mitochondria protein extracts with anti-Aβ and subsequently subjecting them to immunoblotting with anti-ABAD immunoglobulin G. Representative images and quantification of the ABAD–Aβ complex expression was shown. Results are representative of 3 APP/PS1 mice from each group. $^{***}p < 0.001$. Abbreviations: Aβ, β-amyloid; HupA, huperzine A; ABAD, amyloid-binding alcohol dehydrogenase.

to analyze cleaved caspase-3 protein levels via Western blotting. Cleaved caspase-3 levels of the APP/PS1-vehicle group showed significant increases compared with the WT-vehicle control group ($p < 0.001$, Fig. 5B and C). However, the administration of HupA but not tacrine ($p > 0.1$, Fig. 5B and C) to APP/PS1 mice abolished this increase ($p < 0.01$, Fig. 5B and C). Our data suggest that HupA effectively reduced cell apoptosis by inhibiting the release of cytochrome c from mitochondria, as well as the level of caspase-3 in the brain of APP/PS1 mice.

3.6. HupA alleviated DBC damage in APP/PS1 mice

To determine the neuroprotective effect of HupA on APP/PS1 mice, the DBCs from each group were seeded into poly-L-lysine precoated 96-well plates (2×10^4 cells per well) for 24 hours, followed by the LDH and MTT assays. First, the LDH levels of the APP/PS1 mice significantly increased compared with the age-matched WT-vehicle group ($p < 0.001$, Fig. 6A). In addition, HupA but not tacrine treatment ($p > 0.1$, Fig. 6A) markedly decreased LDH levels compared with the APP/PS1 mice without HupA ($p < 0.01$, Fig. 6A). The DBCs LDH levels of the WT mice treated with HupA did not change compared with the WT-vehicle control group ($p > 0.1$, Fig.6A).

We next investigated the effect of HupA on cellular metabolic activity and found that in addition to markedly increased LDH levels, the APP/PS1 mice also showed a significant decrease in MTT reduction compared with the age-matched WT-vehicle group ($p < 0.01$, Fig. 6B). Furthermore, HupA treatment but not tacrine treatment ($p > 0.1$, Fig. 6B) resulted in a significant increase in MTT reduction compared with APP/PS1 mice without HupA ($p < 0.01$, Fig. 6B). Interestingly, the MTT reduction of the WT mice treated with HupA group was not significantly different from the WT-vehicle control group ($p > 0.1$, Fig. 6B).

4. Discussion

HupA is a China Food and Drug Administration–approved AD drug that is widely used clinically in China and is undergoing preclinical testing in the United States (Zhu et al., 2015). HupA is increasingly considered a very promising therapeutic agent against AD with potential disease-modifying characteristics (Damar et al., 2017; Zhang, 2012). HupA can readily pass through the blood–brain barrier (Patocka, 1998), therefore in this study, it was administered by intraperitoneal injection rather than intracranial injection to reduce the damage caused by experimental manipulation to the brains of AD mice.

Because HupA exhibits reversible AChE inhibitor properties, we used another classical AChE inhibitor called tacrine for comparison, to better illustrate that the mitochondrial protective effects of HupA are non-AChEI dependent. Furthermore, the results of the AChE activity assay in the present study suggest that the inhibitory effects of HupA and tacrine are equivalent.

In the present study, we explored the role of mitochondria in the process of neuroprotective effect by HupA in APP/PS1 mice. In addition, results showed that a reduction in the levels of ABAD is associated with the protection of brain mitochondria by HupA in vivo.

Aβ proteins, especially those comprising 42 amino acids (Aβ42), are widely recognized as the main neurotoxic species responsible for the development of AD (Eleuteri et al., 2015; Selkoe and Schenk, 2003). A plethora of studies have shown that there is a large

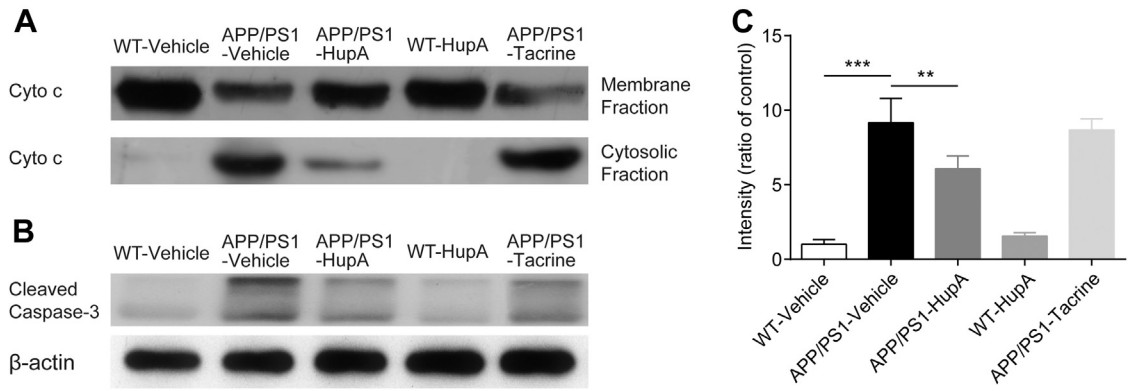

Fig. 5. HupA effectively reduced cytochrome c release from the mitochondrial or membrane fraction into the cytoplasm and decreased the levels of cleaved caspase-3 in acutely prepared DBCs of APP/PS1 mice. (A) Cytosol and membrane proteins were separated from acutely prepared DBCs and then analyzed, and the subcellular distribution of cytochrome c was detected by Western blot. (B) Representative images of cleaved caspase-3 were analyzed by Western blotting. (C) Quantitative analysis of the band intensity of cleaved caspase-3. $^{**}p < 0.01$, $^{***}p < 0.001$. Abbreviations: HupA, huperzine A; DBCs, dissociated brain cells.

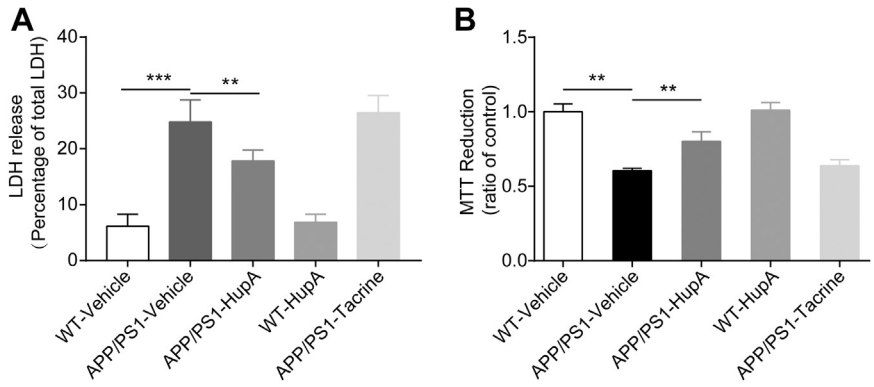

Fig. 6. Huperzine A alleviated DBC damage in APP/PS1 mice. (A). DBCs from each group (n = 8) were seeded into poly-L-lysine precoated 96-well plates (2×10^4 cells per well) for 24 hours, the supernatant was harvested to test the LDH release according to the manufacturer's protocols. Similarly, after the DBCs were seeded into poly-L-lysine pre-coated 96-well plates (2×10^4 cells per well) for 24 hours, Triton X-100 (10%) was added and incubated for 1 hour in an incubator, and the supernatant was collected to measure the total LDH. Data are presented as percentage of total LDH and shown as mean ± SEM. (B) DBCs were seeded into 96-well plates (2×10^4 cells per well) and incubated in culture medium for 24 hours, followed by the MTT assay (n = 8). Data are presented as fold-change from the control group and shown as mean ± SEM. $^{**}p < 0.01$, $^{***}p < 0.001$. Abbreviations: DBCs, dissociated brain cells; LDH, lactate dehydrogenase; MTT, 3-(4,5-dimethylthiazol-2-yl)-2,5-diphenyltetrazolium bromide.

amount of Aβ plaque formation in the cortex and hippocampi of the brains of patients with AD and transgenic AD mouse models (Caspersen et al., 2005; Lustbader, 2004; Manczak et al., 2006). In this study, both thioflavin S immunostaining and Western blotting results (Fig. 2) confirmed that there is a significantly increased level of Aβ in the brains of 8-month-old transgenic APP/PS1 mice.

Previous studies have confirmed that Aβ-induced neuronal mitochondrial dysfunction is the main pathogenic mechanism that causes AD (Du et al., 2008; Lustbader, 2004; Reddy and Beal, 2008; Takuma et al., 2005). Although Aβ can directly induce mitochondrial lesions (Crouch et al., 2005; Hernandez-Zimbron et al., 2012), the combination of Aβ and ABAD is increasingly recognized as a major cause of mitochondrial stress and neuronal cell death (Lustbader, 2004; Takuma et al., 2005; Valaasani et al., 2014; Zakaria et al., 2016). The binding of Aβ to ABAD inhibits the enzyme activity of ABAD, which plays an essential role in maintaining a steady state of mitochondrial energy production, and causes mitochondrial ROS overload and insufficient ATP production (Simpkins et al., 2010; Yan et al., 1997, 1999). In addition, segregating ABAD from Aβ protects mitochondria/neurons from Aβ toxicity, and ABAD-Aβ interaction is an important mechanism underlying Aβ-mediated mitochondrial and neuronal perturbation. Inhibitors of ABAD-Aβ interaction may hold promise as targets for the prevention and treatment of AD (Yao et al., 2011). A recent research has highlighted that the presequence protease, a mitochondrial peptidasome, could act as a novel mitochondrial Aβ degrading enzyme, and attenuate AD-like mitochondrial amyloid pathology, synaptic mitochondrial dysfunction, improve learning and memory and synaptic function in vivo AD mice, and alleviates Aβ-mediated reduction of long-term potentiation (Fang et al., 2015). To evaluate whether HupA protects against mitochondrial malfunction in APP/PS1 transgenic mice, we tested mitochondrial ROS and ATP production of DBCs in APP/PS1 mice treated with or without HupA or tacrine. Our data indicated there was a significant increase in ROS and ATP levels in the DBCs of APP/PS1 mice without HupA treatment. However, HupA treatment showed a protective effect on mitochondria by decreasing ROS levels and increasing ATP production. Similar results have been described in previous studies (Gao et al., 2009; Lei et al., 2015; Zhu et al., 2015). Moreover, Yang et al. (2012) showed that HupA protected against oligomeric $A\beta_{1-42}$-mediated isolated mitochondrial ATP reduction, attributing the effect to an increase in the enzymatic activities of respiratory chain complexes in APP/PS1 double transgenic mice. Tao et al. (2016) also showed that HupA ameliorated iron overload–induced oxidative damage to mitochondria by decreasing ROS production and increasing ATP levels in primary cortical neuron. Furthermore, Gao et al. (2009) found that HupA reduced mitochondrial ROS production and increased ATP levels in Aβ-treated PC12 cells. Regrettably, the protective effect on mitochondrial function was not found in the tacrine treatment group. In accordance with our results, Tsang et al. (2006) confirmed that tacrine has no neuroprotective effect on $A\beta_{25-35}$-induced primary cortical neuron death.

To explore the exact mechanism by which HupA attenuates mitochondrial damage in the brain of APP/PS1 mice, we first investigated the involvement of Aβ. Western blotting data demonstrated increased levels of $A\beta_{1-42}$ oligomers (27 kDa) in APP/PS1 mice. Interestingly, it has been reported that these types of Aβ oligomers, referred to as Aβ-derived diffusible ligands, can diffuse into cells and enhance mitochondrial toxicity as they are considered a form of Aβ oligomers with high neurotoxicity (Lambert et al., 1998). Moreover, Lei et al. (2015) showed that $A\beta_{1-42}$ accumulates intraneuronally in a dose- and time-dependent manner. This group further reported that the level of intracellular $A\beta_{1-42}$ is correlated with mitochondrial function and cell viability in primary rat neurons in vitro, whereas HupA treatment decreased the mitochondrial accumulation of $A\beta_{1-42}$ and mitigated mitochondrial damage. Similarly, immunohistochemistry and Western blotting data in the present study showed that HupA treatment decreased the level of Aβ in the brain of APP/PS1 mice. In addition, our findings are in accordance with Huang et al. (2014), who found that HupA treatment reduced Aβ levels and ameliorated Aβ plaque formation in the cortex and hippocampi of transgenic APPswe/PS1dE9 mice. Alternatively, tacrine showed no ability to reduce Aβ level. The previous study led by Chang et al. (2015) also suggested that tacrine minimally attenuated the accumulation of Aβ, even at a very high concentration.

However, it is not yet clear how $A\beta_{1-42}$ damages mitochondrial function. Recent studies reported that ABAD was overexpressed in the cerebral cortex and hippocampi of patients with AD and amyloid precursor protein (APP/Aβ)-overexpressing transgenic mice (Chen and Yan, 2007; Cuadrado-Tejedor et al., 2013; Yao et al., 2009). Studies have also reported that ABAD exacerbates Aβ-induced mitochondrial dysfunction and neurotoxicity in patients with AD and the transgenic AD mouse model (Lustbader, 2004; Takuma et al., 2005; Valaasani et al., 2014). The combination of

Aβ and ABAD induces structural abnormalities in ABAD, which impedes the binding of ABAD to NAD^+. NAD^+ is a coenzyme that assists ABAD in the regulation of mitochondrial physiological function (Lustbader, 2004). In addition, AG18051 (an ABAD inhibitor) conferred resistance to Aβ-mediated mitochondrial injury in SH-SY5Y neuroblastoma cells (Lim et al., 2011). Studies have shown that ABAD-DPs protect against Aβ-mediated mitochondrial toxicity in the neurons of Tg ABAD mice (Lustbader, 2004). These results suggest that ABAD plays an indispensable role in the pathogenesis of AD. Our study further explored whether ABAD contributes to the protective effects of HupA on brain mitochondria. We found that ABAD expression levels were significantly increased in the brain tissue obtained from APP/PS1 mice compared with the age-matched WT mice, whereas APP/PS1 mice treated with HupA showed dramatically decreased ABAD protein levels. To further investigate the effect of HupA on ABAD protein level, we stimulated PC12 cells with Aβ in vitro and found that ABAD levels were significantly elevated; however, HupA treatment effectively reversed this increase. Alternatively, tacrine had no effect on ABAD levels in APP/PS1 mice and PC12 cells. These findings suggested that HupA but not tacrine can reduce ABAD protein expression. Hence, for the first time, we demonstrated that ABAD is associated with the protective effects of HupA on mitochondria in vivo.

Finally, we investigated whether the combination of Aβ and ABAD is associated with the protective effects of HupA on brain mitochondria. Coimmunoprecipitation results showed that complex formation of Aβ and ABAD was significantly increased in AD mice, whereas HupA significantly reduced complex formation. Together, these results showed that HupA significantly reduced ABAD protein levels in APP/PS1 mice, although it did not completely recover WT levels, and HupA reduced the level of Aβ, thus reducing the level of Aβ-ABAD compound.

The combination of Aβ and ABAD results in the release of cytochrome c from the mitochondria to the cytoplasm, which subsequently triggers the caspase-3-dependent apoptotic pathway (Lim et al., 2011; Lustbader, 2004; Takuma et al., 2005). Cytochrome c is a proapoptotic factor that binds to apoptotic protease activating factor-1, resulting in the cleavage of caspase-3, DNA degradation, and cell death (D'Amelio et al., 2011; Morais et al., 2002). Lustbader (2004) utilized an ABAD-DP that inhibits the binding of Aβ to ABAD to protect against Aβ-mediated mitochondrial cytochrome c release in neurons from Tg ABAD mice. Consistent with previous research (Lustbader, 2004), our data suggest that a significant amount of cytochrome c protein is released from the mitochondria into the cytoplasm, and the level of cleaved caspase-3 is increased in the brain of APP/PS1 mice. However, APP/PS1 mice treated with HupA exhibited an inhibition of the release of cytochrome c and reduced levels of cleaved caspase-3. Our results are supported by previous research by Gao et al. (2009) who showed that HupA reduced the Aβ-induced leakage of cytochrome c from the isolated rat brain mitochondria. Furthermore, we observed that DBCs injury in APP/PS1 mice is dramatically increased compared with WT mice, which was confirmed by an increase in LDH level and a decrease in the MTT reduction. However, HupA significantly decreased the level of LDH and significantly increased the MTT reduction in DBCs obtained from APP/PS1 mice, suggesting that DBCs viability was greatly improved. Consistent with previous studies, no neuroprotective effect has been observed with tacrine, suggesting that tacrine does not decrease neuronal cell death in vitro (Tsang et al., 2006).

In the present study, DBCs isolated from brain of APP/PS1 mice contained all types of brain cells, which could realistically mimic brain homeostasis. Therefore, the use of DBCs for in vitro experiments can more practically reflect the relationship between HupA and ABAD protein in APP/PS1 mice brain. It seems unlikely that the percentages of various neuronal subtypes and glial types of DBCs differ much across the experimental groups; however, there could in fact be differences across groups since the complexity of cell types and their percentages were not evaluated. Although it may not be optimal to use DBCs for in vitro experiments at present stage, it should be sufficient to draw a conclusion that HupA protects mitochondrial function by reducing ABAD protein levels. Future research will explore more appropriate experimental parameters to assess the complexity of cell types and their percentages of DBCs.

In conclusion, HupA prevents Aβ-ABAD-induced neurotoxicity by reducing ABAD levels, thereby improving mitochondrial function and enhancing DBCs viability in APP/PS1. Our results revealed the mechanism behind the pharmacological action of HupA in the treatment of AD in a non-AChEI-dependent pathway and provide a novel therapeutic approach for the further elucidation of the role of HupA in the treatment of AD. Because HupA reduces the level of oligomeric Aβ, which was reported to be directly involved in synaptic toxicity and cognitive dysfunction in the early stages of AD (Benilova et al., 2012), it may also be used to prevent the onset in those with a family history of AD, and to slow the progression of those with early signs of the disease. Future studies will examine whether HupA directly inhibits the binding of Aβ and ABAD.

Disclosure

The authors have no actual or potential conflicts of interest.

Acknowledgements

This study was supported in part by grants from the National Natural Science Foundation of China (No. 3097162) and the National Natural Science Foundation of Guangdong Province (No. S2013010015546). The authors would like to thank LetPub (www.letpub.com) for providing linguistic assistance during the preparation of this article.

Appendix A. Supplementary data

Supplementary data to this article can be found online at https://doi.org/10.1016/j.neurobiolaging.2019.05.016.

References

Abdel-Kader, R., Hauptmann, S., Keil, U., Scherping, I., Leuner, K., Eckert, A., Muller, W.E., 2007. Stabilization of mitochondrial function by Ginkgo biloba extract (EGb 761). Pharmacol. Res. 56, 493–502.

Aitken, L., Baillie, G., Pannifer, A., Morrison, A., Jones, P.S., Smith, T.K., McElroy, S.P., Gunn-Moore, F.J., 2017. In vitro assay development and HTS of small-molecule human ABAD/17beta-HSD10 inhibitors as therapeutics in Alzheimer's disease. SLAS Discov. 22, 676–685.

Aitken, L., Quinn, S.D., Perez-Gonzalez, C., Samuel, I.D.W., Penedo, J.C., Gunn-Moore, F.J., 2016. Morphology-Specific inhibition of β-amyloid aggregates by 17β-hydroxysteroid dehydrogenase type 10. Chembiochem 17, 1029–1037.

Amtul, Z., Wang, L., Westaway, D., Rozmahel, R.F., 2010. Neuroprotective mechanism conferred by 17beta-estradiol on the biochemical basis of Alzheimer's disease. Neuroscience 169, 781–786.

Asseburg, H., Schafer, C., Muller, M., Hagl, S., Pohland, M., Berressem, D., Borchiellini, M., Plank, C., Eckert, G.P., 2016. Effects of grape skin extract on age-related mitochondrial dysfunction, memory and life span in C57BL/6J mice. Neuromolecular Med. 18, 378–395.

Benek, O., Aitken, L., Hroch, L., Kuca, K., Gunn-Moore, F., Musilek, K., 2015. A direct interaction between mitochondrial proteins and amyloid-β peptide and its significance for the progression and treatment of Alzheimer's disease. Curr. Med. Chem. 22, 1056–1085.

Benek, O., Hroch, L., Aitken, L., Gunn-Moore, F., Vinklarova, L., Kuca, K., Perez, D.I., Perez, C., Martinez, A., Fisar, Z., Musilek, K., 2018. 1-(Benzo[d]thiazol-2-yl)-3-phenylureas as dual inhibitors of casein kinase 1 and ABAD enzymes for treatment of neurodegenerative disorders. J. Enzyme Inhib. Med. Chem. 33, 665–670.

Benilova, I., Karran, E., De, B.S., 2012. The toxic Aβ oligomer and Alzheimer's disease: an emperor in need of clothes. Nat. Neurosci. 15, 349.

Caspersen, C., Wang, N., Yao, J., Sosunov, A., Chen, X., Lustbader, J.W., Xu, H.W., Stern, D., McKhann, G., Yan, S.D., 2005. Mitochondrial Abeta: a potential focal point for neuronal metabolic dysfunction in Alzheimer's disease. FEBS J. 19, 2040–2041.

Cha, M.Y., Han, S.H., Son, S.M., Hong, H.S., Choi, Y.J., Byun, J., Mook-Jung, I., 2012. Mitochondria-specific accumulation of amyloid beta induces mitochondrial dysfunction leading to apoptotic cell death. PLoS One 7, e34929.

Chang, L., Cui, W., Yang, Y., Xu, S., Zhou, W., Fu, H., Hu, S., Mak, S., Hu, J., Wang, Q., 2015. Protection against β-amyloid-induced synaptic and memory impairments via altering β-amyloid assembly by bis(heptyl)-cognitin. Sci. Rep. 5, 10256.

Chen, J.X., Yan, S.D., 2007. Amyloid-beta-induced mitochondrial dysfunction. J. Alzheimers Dis. 12, 177–184.

Chen, Q., Wang, K., Jiang, D., Wang, Y., Xiao, X., Zhu, N., Li, M., Jia, S., Wang, Y., 2016. Blocking mPTP on neural stem cells and activating the Nicotinic acetylcholine receptor α7 subunit on microglia attenuate Aβ-induced neurotoxicity on neural stem cells. Neurochem. Res. 41, 1483–1495.

Crouch, P.J., Blake, R., Duce, J.A., Ciccotosto, G.D., Li, Q.X., Barnham, K.J., Curtain, C.C., Cherny, R.A., Cappai, R., Dyrks, T., Masters, C.L., Trounce, I.A., 2005. Copper-dependent inhibition of human cytochrome c oxidase by a dimeric conformer of amyloid-beta1-42. J. Neurosci. 25, 672–679.

Cuadrado-Tejedor, M., Cabodevilla, J.F., Zamarbide, M., Gomez-Isla, T., Franco, R., Perez-Mediavilla, A., 2013. Age-related mitochondrial alterations without neuronal loss in the hippocampus of a transgenic model of Alzheimer's disease. Curr. Alzheimer Res. 10, 390–405.

Damar, U., Gersner, R., Johnstone, J.T., Schachter, S., Rotenberg, A., 2017. Huperzine A: a promising anticonvulsant, disease modifying, and memory enhancing treatment option in Alzheimer's disease. Med. Hypotheses 99, 57–62.

D'Amelio, M., Cavallucci, V., Middei, S., Marchetti, C., Pacioni, S., Ferri, A., Diamantini, A., De Zio, D., Carrara, P., Battistini, L., Moreno, S., Bacci, A., Ammassari-Teule, M., Marie, H., Cecconi, F., 2011. Caspase-3 triggers early synaptic dysfunction in a mouse model of Alzheimer's disease. Nat. Neurosci. 14, 69–76.

Dragicevic, N., Mamcarz, M., Zhu, Y., Buzzeo, R., Tan, J., Arendash, G.W., Bradshaw, P.C., 2010. Mitochondrial amyloid-beta levels are associated with the extent of mitochondrial dysfunction in different brain regions and the degree of cognitive impairment in Alzheimer's transgenic mice. J. Alzheimers Dis. 20 (Suppl.2), S535–S550.

Du, H., Guo, L., Fang, F., Chen, D., A Sosunov, A., M McKhann, G., Yan, Y., Wang, C., Zhang, H., Molkentin, J.D., Gunn-Moore, F.J., Vonsattel, J.P., Arancio, O., Chen, J.X., Yan, S.D., 2008. Cyclophilin D deficiency attenuates mitochondrial and neuronal perturbation and ameliorates learning and memory in Alzheimer's disease. Nat. Med. 14, 1097–1105.

Eleuteri, S., Di Giovanni, S., Rockenstein, E., Mante, M., Adame, A., Trejo, M., Wrasidlo, W., Wu, F., Fraering, P.C., Masliah, E., Lashuel, H.A., 2015. Novel therapeutic strategy for neurodegeneration by blocking Abeta seeding mediated aggregation in models of Alzheimer's disease. Neurobiol. Dis. 74, 144–157.

Ellman, G.L., Courtney, K.D., Jr, A.V., Featherstone, R.M., 1961. A new and rapid colorimetric determination of acetylcholinesterase activity. Biochem. Pharmacol. 7, 88–95.

Fang, D., Wang, Y., Zhang, Z., Du, H., Yan, S., Sun, Q., Zhong, C., Wu, L., Vangavaragu, J.R., Yan, S., Hu, G., Guo, L., Rabinowitz, M., Glaser, E., Arancio, O., Sosunov, A.A., McKhann, G.M., Chen, J.X., Yan, S.S., 2015. Increased neuronal PreP activity reduces Aβ accumulation, attenuates neuroinflammation and improves mitochondrial and synaptic function in Alzheimer disease's mouse model. Hum. Mol. Genet. 24, 5198–5210.

Gao, X., Zheng, C.Y., Yang, L., Tang, X.C., Zhang, H.Y., 2009. Huperzine A protects isolated rat brain mitochondria against β-amyloid peptide. Free Radic. Biol. Med. 46, 1454–1462.

Grimm, A., Lim, Y.A., Mensah-Nyagan, A.G., Gotz, J., Eckert, A., 2012. Alzheimer's disease, oestrogen and mitochondria: an ambiguous relationship. Mol. Neurobiol. 46, 151–160.

Halestrap, A., 2005. Biochemistry: a pore way to die. Nature 434, 578–579.

Heneka, M.T., Kummer, M.P., Stutz, A., Delekate, A., Schwartz, S., Vieira-Saecker, A., Griep, A., Axt, D., Remus, A., Tzeng, T., Gelpi, E., Halle, A., Korte, M., Latz, E., Golenbock, D.T., 2012. NLRP3 is activated in Alzheimer's disease and contributes to pathology in APP/PS1 mice. Nature 493, 674–678.

Hernandez-Zimbron, L.F., Luna-Munoz, J., Mena, R., Vazquez-Ramirez, R., Kubli-Garfias, C., Cribbs, D.H., Manoutcharian, K., Gevorkian, G., 2012. Amyloid-beta peptide binds to cytochrome C oxidase subunit 1. PLoS One 7, e42344.

Hirai, K., Aliev, G., Nunomura, A., Fujioka, H., Russell, R.L., Atwood, C.S., Johnson, A.B., Kress, Y., Vinters, H.V., Tabaton, M., Shimohama, S., Cash, A.D., Siedlak, S.L., Harris, P.L., Jones, P.K., Petersen, R.B., Perry, G., Smith, M.A., 2001. Mitochondrial abnormalities in Alzheimer's disease. J. Neurosci. 21, 3017–3023.

Hroch, L., Benek, O., Guest, P., Aitken, L., Soukup, O., Janockova, J., Musil, K., Dohnal, V., Dolezal, R., Kuca, K., Smith, T.K., Gunn-Moore, F., Musilek, K., 2016. Design, synthesis and in vitro evaluation of benzothiazole-based ureas as potential ABAD/17beta-HSD10 modulators for Alzheimer's disease treatment. Bioorg. Med. Chem. Lett. 26, 3675–3678.

Hroch, L., Guest, P., Benek, O., Soukup, O., Janockova, J., Dolezal, R., Kuca, K., Aitken, L., Smith, T.K., Gunn-Moore, F., Zala, D., Ramsay, R.R., Musilek, K., 2017. Synthesis and evaluation of frentizole-based indolyl thiourea analogues as MAO/ABAD inhibitors for Alzheimer's disease treatment. Bioorg. Med. Chem. 25, 1143–1152.

Huang, X., Qian, Z., He, X., Gong, Q., Wu, K., Jiang, L., Lu, L., Zhu, Z., Zhang, H., Yung, W., Ke, Y., 2014. Reducing iron in the brain: a novel pharmacologic mechanism of huperzine A in the treatment of Alzheimer's disease. Neurobiol. Aging 35, 1045–1054.

Lambert, M.P., Barlow, A.K., Chromy, B.A., Edwards, C., Freed, R., Liosatos, M., Morgan, T.E., Rozovsky, I., Trommer, B., Viola, K.L., Wals, P., Zhang, C., Finch, C.E., Krafft, G.A., Klein, W.L., 1998. Diffusible, nonfibrillar ligands derived from Aβ1–42 are potent central nervous system neurotoxins. Proc. Natl. Acad. Sci. U. S. A. 95, 6448–6453.

Lei, Y., Yang, L., Ye, C.Y., Qin, M.Y., Yang, H.Y., Jiang, H.L., Tang, X.C., Zhang, H.Y., 2015. Involvement of intracellular and mitochondrial Aβ in the ameliorative effects of huperzine a against oligomeric Aβ42-induced injury in primary rat neurons. PLoS One 10, e128366.

Lim, Y.A., Grimm, A., Giese, M., Mensah-Nyagan, A.G., Villafranca, J.E., Ittner, L.M., Eckert, A., Gotz, J., 2011. Inhibition of the mitochondrial enzyme ABAD restores the amyloid-beta-mediated deregulation of estradiol. PLoS One 6, e28887.

Liu, Y., Liu, W., Song, X.D., Zuo, J., 2005. Effect of GRP75/mthsp70/PBP74/mortalin overexpression on intracellular ATP level, mitochondrial membrane potential and ROS accumulation following glucose deprivation in PC12 cells. Mol. Cell. Biochem. 268, 45–51.

Lustbader, J.W., 2004. ABAD directly links Aβ to mitochondrial toxicity in Alzheimer's disease. Science 304, 448–452.

Manczak, M., Anekonda, T.S., Henson, E., Park, B.S., Quinn, J., Reddy, P.H., 2006. Mitochondria are a direct site of A beta accumulation in Alzheimer's disease neurons: implications for free radical generation and oxidative damage in disease progression. Hum. Mol. Genet. 15, 1437–1449.

Morais, C.S., Swerdlow, R.H., Oliveira, C.R., 2002. Induction of cytochrome c-mediated apoptosis by amyloid beta 25-35 requires functional mitochondria. Brain Res. 931, 117–125.

Pagani, L., Eckert, A., 2011. Amyloid-Beta interaction with mitochondria. Int. J. Alzheimers Dis. 2011, 925050.

Patocka, J., 1998. Huperzine A–an interesting anticholinesterase compound from the Chinese herbal medicine. Acta Medica 41, 155–157.

Pohland, M., Pellowska, M., Asseburg, H., Hagl, S., Reutzel, M., Joppe, A., Berressem, D., Eckert, S.H., Wurglics, M., Schubert-Zsilavecz, M., Eckert, G.P., 2018. MH84 improves mitochondrial dysfunction in a mouse model of early Alzheimer's disease. Alzheimers Res. Ther. 10, 18.

Readnower, R.D., Sauerbeck, A.D., Sullivan, P.G., 2011. Mitochondria, amyloid beta, and Alzheimer's disease. Int. J. Alzheimers Dis. 2011, 104545.

Reddy, P.H., Beal, M.F., 2008. Amyloid beta, mitochondrial dysfunction and synaptic damage: implications for cognitive decline in aging and Alzheimer's disease. Trends Mol. Med. 14, 45–53.

Rhein, V., Baysang, G., Rao, S., Meier, F., Bonert, A., Muller-Spahn, F., Eckert, A., 2009. Amyloid-beta leads to impaired cellular respiration, energy production and mitochondrial electron chain complex activities in human neuroblastoma cells. Cell. Mol. Neurobiol. 29, 1063–1071.

Sakono, M., Zako, T., 2010. Amyloid oligomers: formation and toxicity of Abeta oligomers. FEBS J. 277, 1348–1358.

Sanz-Blasco, S., Valero, R.A., Rodriguez-Crespo, I., Villalobos, C., Nunez, L., 2008. Mitochondrial Ca2+ overload underlies Abeta oligomers neurotoxicity providing an unexpected mechanism of neuroprotection by NSAIDs. PLoS One 3, e2718.

Selkoe, D.J., 2007. Developing preventive therapies for chronic diseases: lessons learned from Alzheimer's disease. Nutr. Rev. 65, S239–S243.

Selkoe, D.J., Schenk, D., 2003. Alzheimer's disease: molecular understanding predicts amyloid-based therapeutics. Annu. Rev. Pharmacol. 43, 545–584.

Simpkins, J.W., Yi, K.D., Yang, S.H., Dykens, J.A., 2010. Mitochondrial mechanisms of estrogen neuroprotection. Biochim. Biophys. Acta 1800, 1113–1120.

Stoll, L., Schubert, T., Muller, W.E., 1992. Age-related deficits of central muscarinic cholinergic receptor function in the mouse: partial restoration by chronic piracetam treatment. Neurobiol. Aging 13, 39–44.

Takuma, K., Yao, J., Huang, J., Xu, H., Chen, X., Luddy, J., Trillat, A.C., Stern, D.M., Arancio, O., Yan, S.S., 2005. ABAD enhances Abeta-induced cell stress via mitochondrial dysfunction. FASEB J. 19, 597–598.

Tao, L.X., Huang, X.T., Chen, Y.T., Tang, X.C., Zhang, H.Y., 2016. Acetylcholinesterase-independent protective effects of huperzine A against iron overload-induced oxidative damage and aberrant iron metabolism signaling in rat cortical neurons. Acta Pharmacol. Sin. 37, 1391–1400.

Tsang, H.W., Pang, Y., Chang, D.C., 2006. Bis(7)-tacrine attenuates beta amyloid-induced neuronal apoptosis by regulating L-type calcium channels. J. Neurochem. 98, 1400–1410.

Valaasani, K.R., Sun, Q., Hu, G., Li, J., Du, F., Guo, Y., Carlson, E.A., Gan, X., Yan, S.S., 2014. Identification of human ABAD inhibitors for rescuing Abeta-mediated mitochondrial dysfunction. Curr. Alzheimer Res. 11, 128–136.

Voloboueva, L.A., Lee, S.W., Emery, J.F., Palmer, T.D., Giffard, R.G., 2010. Mitochondrial protection attenuates inflammation-induced impairment of neurogenesis in vitro and in vivo. J. Neurosci. 30, 12242–12251.

Yan, S.D., Fu, J., Soto, C., Chen, X., Zhu, H., Al-Mohanna, F., Collison, K., Zhu, A., Stern, E., Saido, T., Tohyama, M., Ogawa, S., Roher, A., Stern, D., 1997. An intracellular protein that binds amyloid-beta peptide and mediates neurotoxicity in Alzheimer's disease. Nature 389, 689–695.

Yan, S.D., Shi, Y., Zhu, A., Fu, J., Zhu, H., Zhu, Y., Gibson, L., Stern, E., Collison, K., Al-Mohanna, F., Ogawa, S., Roher, A., Clarke, S.G., Stern, D.M., 1999. Role of ERAB/L-3-hydroxyacyl-coenzyme A dehydrogenase type II activity in Abeta-induced cytotoxicity. J. Biol. Chem. 274, 2145–2156.

Yao, J., Du, H., Yan, S., Fang, F., Wang, C., Lue, L.F., Guo, L., Chen, D., Stern, D.M., Gunn Moore, F.J., Xi Chen, J., Arancio, O., Yan, S.S., 2011. Inhibition of amyloid-beta (Abeta) peptide-binding alcohol dehydrogenase-Abeta interaction reduces

Abeta accumulation and improves mitochondrial function in a mouse model of Alzheimer's disease. J. Neurosci. 31, 2313–2320.
Yang, L., Ye, C.Y., Huang, X.T., Tang, X.C., Zhang, H.Y., 2012. Decreased accumulation of subcellular amyloid-beta with improved mitochondrial function mediates the neuroprotective effect of huperzine A. J. Alzheimers Dis. 31, 131–142.
Yao, J., Irwin, R.W., Zhao, L., Nilsen, J., Hamilton, R.T., Brinton, R.D., 2009. Mitochondrial bioenergetic deficit precedes Alzheimer's pathology in female mouse model of Alzheimer's disease. Proc. Natl. Acad. Sci. U. S. A. 106, 14670–14675.
Zakaria, A., Hamdi, N., Abdel-Kader, R.M., 2016. Methylene blue improves brain mitochondrial ABAD functions and decreases Aβ in a neuroinflammatory Alzheimer's disease mouse model. Mol. Neurobiol. 53, 1220–1228.
Zhang, H.Y., 2012. New insights into huperzine A for the treatment of Alzheimer's disease. Acta Pharmacol. Sin. 33, 1170–1175.
Zhu, N., Lin, J., Wang, K., Wei, M., Chen, Q., Wang, Y., 2015. Huperzine A protects neural stem cells against Abeta-induced apoptosis in a neural stem cells and microglia co-culture system. Int. J. Clin. Exp. Pathol. 8, 6425–6433.